 MCB, vol.13, no.1, pp.23-36, 2016

The Correlation Between Texture Features and Fibrous Cap Thickness of Lipid-Rich Atheroma Based on Optical Coherence Tomography Imaging

Chunliu He[1], Jiaqiu Wang[2], Yuxiang Huang[1], Tongjing Zhu[1], Yuehong Miao[1], Zhiyong Li[1,2*]

Abstract: Fibrous cap thickness (FCT) is seen as critical to plaque vulnerability. Therefore, the development of automatic algorithms for the quantification of FCT is for estimating cardiovascular risk of patients. Intravascular optical coherence tomography (IVOCT) is currently the only *in vivo* imaging modality with which FCT, the critical component of plaque vulnerability, can be assessed accurately.This study was aimed to discussionthecorrelation between the texture features of OCT images and the FCT in lipid-rich atheroma.Firstly, a full automatic segmentation algorithm based on unsupervised fuzzy c means(FCM) clustering with geometric constrains was developed to segment the ROIs of IVOCT images. Then, 32 features, which are associated with the structural and biochemical changes of tissue, were carried out to describe the properties of ROIs. The FCT in grayscale IVOCT images were manually measured by two independent observers. In order to analysis the correlationbetweenIVOCT image features and manual FCT measurements, linear regression approach was performed. Inter-observer agreement of the twice manual FCT measurements was excellent with an intraclass correlation coefficient (ICC) of 0.99.The correlation coefficient between each individual feature set and mean FCT of OCT images were 0.68 for FOS, 0.80 for GLCM, 0.74 for NGTDM, 0.72 for FD, 0.62 for IM and 0.58 for SP. The fusion image features of automatic segmented ROIs and FCT measurements improved the results significantly with a high correlation coefficient (r= 0.91, p<0.001). To conclude, the OCT images features demonstrated the perfect performances and could be used for automatic qualitative analysis and the identification of high-risk plaques instead manual FCT measurements.

Keywords: Atherosclerotic plaque, intravascular optical coherence tomography, fibrous cap thickness, coronary plaque vulnerability.

[1]Department of Biomedical Engineering, College of Biological Science and Medical Engineering, Southeast University, No. 2, Sipailou Street, Xuanwu District, Nanjing, 210000, Jiangsu Province, China.

[2]School of Chemistry, Physics and Mechanical Engineering, Science and Engineering Faculty, Queensland University of Technology, 2 George St, Brisbane City, QLD 4000, Australia.

[*]Corresponding author: Zhiyong Li, email:zylicam@gmail.com.

1 Introduction

Coronary atherosclerotic plaque rupture is a major cause of acute coronary syndrome (ACS)[Yonetsu, Kakuta, Lee,et al.(2011);Habara, Nasu, Terashima, et al. (2014); Cardoso, Weinbaum (2014)]. Thin-capped fibroatheroma (TCFA) is recognized as a precursor for plaque rupture. The pathologic features of TCFA are a large lipid-rich necrotic core (the maximum lipid arc>90^{o}), a thin fibrous cap, and macrophage infiltration into the cap[Habara, Nasu, Terashima, et al. (2014); Cardoso, Weinbaum (2014); Di, Yoon , Kato, et al. (2014); Falk , Nakano, Bentzon, et al. (2013);Fujii, Hao, Shibuya, et al. (2015); Jang, Tearney, MacNeill, et al. (2005);Virmani, Burke, Farb, et al. (2006)]. Postmortem studies have shown that a fibrous cap thickness (FCT) (<65um) prone to rupture, the critical threshold was widely accepted [Tearney, Jang, Bouma (2006); Tian, Dauerman,Toma, et al.(2014)]. The composition and morphology of atherosclerotic plaques are considered to be more important in determining the risk of acute syndromes than the degree of luminal stenosis [Wang, Liu, Zhang, et al. (2016)].Therefore, detection and quantification of FCT of lipid-rich atherosclerotic plaque are important for the assessment of plaque vulnerability in order to prevent acute events and monitor interventional treatments.

Intravascular imaging modalities such as intravascular ultrasound (IVUS) and angiography do not have ability to accurately quantify some of the critical components of a vulnerable plaque such as FCT measurements and macrophage content. IVOCT, however, is a unique high axial resolution (~10μm) imaging modality capable of characterizing these important morphological features of atherosclerotic plaque. IVOCT has demonstrated its capacity in the identification and quantification of FCT in clinical practice [Virmani, Burke, Farb, et al. (2006);Jang, Bouma, Kang, et al. (2002); Kubo, Imanishi, Takarada, et al. (2007)].

According to the published consensus standards for IVOCT images, the plaque lipid core is a signal-poor region within an atherosclerotic plaque, with poorly delineated borders, and little or no signal backscattering. Incontrast, the fibrous caphas a relatively homogeneous signal with high backscattering. Several semi-automatic and fully-automatic methods have been used to segment lipid and fibrous components bya supervised segmentation algorithm [Wang, Chamie, Bezerra, et al. (2012);Athanasiou, Bourantas, Rigas, et al. (2014)]. However, the two major drawbacks that hinder such image analysis are: (1) the procedure is cumbersome and time-consuming because of the large number of pixels, and (2) manual segmentation as the gold standardare subject to a certain degree of variability between different analysts. Therefore, an unsupervised method based on FCM algorithm was introduced in the study to resolve the segmentation problem of the poorly delineated borders of the lipid core.

Therefore, in the present study,we determined the correlation coefficient and statistically significant between FCT measurements and IVOCT images features and estimated effect of OCT image features in quantifying FCT indirectly.

2 Materials and methods

2.1 Image dataset

All 33 IVOCT clinical pullbacks of 20 patients were taken from Affiliated Drum Tower Hospital, Nanjing University between December 2015 and December 2016. The IVOCT images were acquired by using a commercially available Fourier Domain OCT (FDOCT) system (2.7F C7-XR, St. Jude Medical, St. Paul, Minnesota) and C7 Dragonfly catheter (St. Jude). The system is equipped with a near-infrared laser light source with a central wavelength of 1310 nm and full-width-at-half-maximum bandwidth of 80 nm. The imaging system provides an axial resolution ~10 um and a lateral resolution of ~30um in biological tissues. Scan parameters were set as 100 frames/sec, 54,000 A-scans/sec, pullback speed of 20 mm/sec, pullback length of ~54.2 mm. This study was approved by the institutional human ethics committee. All the patients have given explicitly informed consent. IVOCT images including lipid-rich plaques from all pullbacks were selected as all databases. Out of these images, only segments containing lipid-rich plaques were selected based on the published consensus standards [Falk, Nakano, Bentzon, et al. (2013)] and the improvement of standard interpretation algorithm [Kini, Vengrenyuk, Yoshimura, et al. (2017)]. Total of 102 images were selected for further analysis. For each plaque, expert observers selected the same images from the IVOCT runs and measured the thinnest FCT two times, from which the final measurement value of FCT was averaged.

2.2 Image pre-processing

Consider the IVOCT images in polar coordinates where the rowis angle and columnis depth as shown in Fig.1(a).Ring-area (RA)and lumen are automatically segmented by the following four steps. The results of each step are shown in Fig.1. The procedures include:

- Remove guide-wire and artifacts;
- The horizontal and vertical thresholdscalculated were taken into account the catheter size of polar image,then, set to the rows and columns to zeros based on the thresholds, the result as follow in Fig.1 (b);
- Binarization images were processed by adaptive threshold Otsu's method algorithm and by morphological connect neighborhood and area constraint [Koga, Ikeda, Yoshida, Nakata, Takeno, Masuda, Koide, Kawano, Maemura (2013)];
- Lumen was automatically segmented by connecting the nonzero pixels, interpolating pixels of full zero row, and then expanding lumen to 1mm to take into account the limited penetration depth of OCT system;
- The polar images were subsequently converted to a cartesian coordinate in order to reconstruct an image that preserved the true vessel wall morphology of visualization.

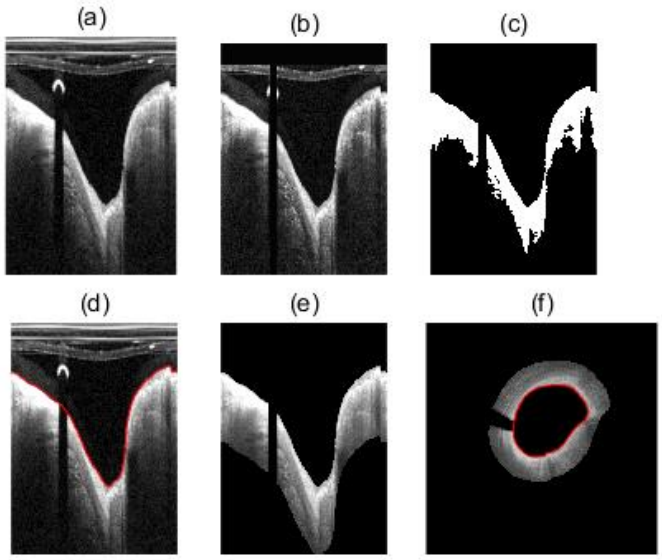

Figure 1: Illustration of the fully-automated segmentation procedure

Image (a) shows original raw polar domain image;Image (b) shows the guide-wire and catheter artifacts removal partially;Image (c) illustrates the application of the Otsu's method, morphological operations and the area constrain;Image (d) shows lumen segmentation result; Image (e) and (f) show the RA segmentation results before and after scan-conversion respectively

2.3 Region of interest(ROI) extraction

Compared to fibrous cap, necrotic lipid core exhibits a lower signal density and a more heterogeneous back-scattering [Prati, Guagliumi, Mintz, et al.(2012);Prati, Regar, Mintz, et al. (2010)]. Lipid core area has the followingmajor characteristics: diffusely bordered, signal-poor regions with overlying signal-rich bands. In this paper, FCM method was selected to extract the cap of fibrous components[Chamie, Bezerra, Attizzani, et al. (2013)], which was contoured with green solid lineas shown in Fig.2 (a). Once the cap of fibrous components was segmented, the lipid core borders were subsequently obtained by arc angle of lumen contours.Thecontourofthe fibrous cap componentin the 2-D image was represented bytwocurves along *x-axis* and y-*axis*in Fig.2 (b) and (c).Asimple polynomial curve fitting algorithmwasproposedin order to smooth two curves. Next, the key problem was to locate the two points pointed by the white arrow to extract ROI.We used the simple geometric constraints: the catheter center set as an origin, four equal regions were divided, the same arc angle in Fig.2 (b) and (c) are the points indicated by white arrow in Fig.2 (a). Fig.3givesthree representative results of the ROI in different pullbacks.

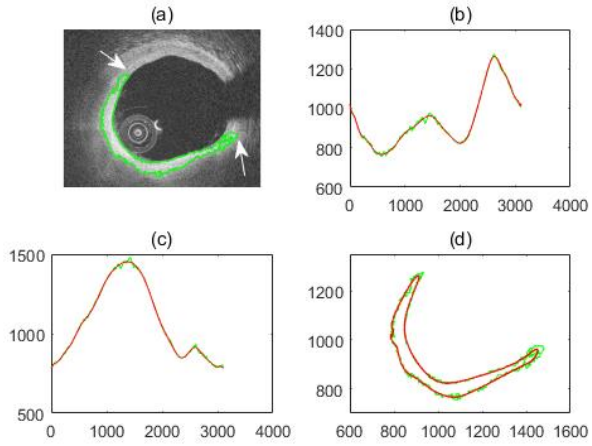

Figure 2: The fibrous cap contour extraction algorithm using the FCM algorithm with geometric constraint

The green solid line contour of image (a) shows the cap segmentation result byFCM algorithm. Image (b) and (c) display the fitting results using polynomial curve fitting algorithm. The green solid line and red solid line represent curve shape of the row and column index valuebefore and after polynomial curve fitting, respectively. Image (d) shows the cap contours of image (a) before and after polynomial curve fitting

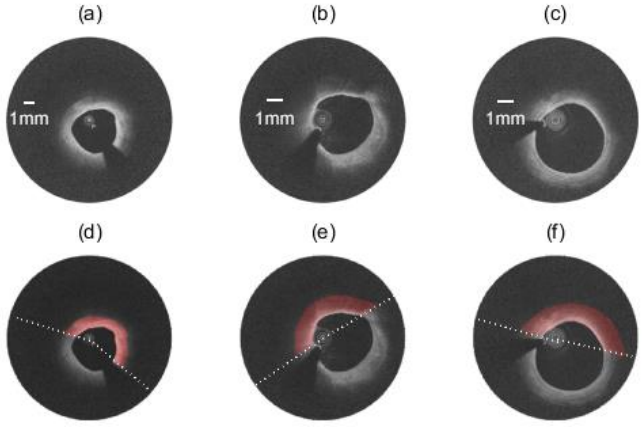

Figure3: Representative results of the ROI on three frames from different pullbacks

Image (a), (b) and (c) show the log image with lipid-rich plaques in the cartesian coordinate. Image (c), (d) and (f) show the ROI (red overlay region) corresponding to the image (a), (b) and (c), respectively

2.4 Feature extraction

Texture features and shape parameters were extracted from ROIs. Texture refers to the spatial interrelationship and arrangement of the basic elements of an image [Kato, Yonetsu, Jia, et al.(2013); Christodoulou, Pattichis, Pantziaris, et al.(2003)]. Texture features have to be derived from the gray images because the spatial interrelationships and the arrangements of the image pixels are seen as variations in the intensity patterns or gray tones visually. Although it is easy to recognize different kinds of textures, it is quite a difficult task to define and interpret the texturesautomatically by computer algorithm.Shape is also an important feature for medical image [Wang, Liu, Zhang, et al. (2016)]. In this paper, six different feature sets composing of a total 32 features were listedin table 1.The implementation details for the texture features, shape parameters and referred papers are shown below:

Table 1: Feature setsinformation and corresponding references

Feature sets	Feature name	Reference
FOS	mean, variance, median, skewness, kurtosis	[Christodoulou, Pattichis, Pantziaris, et al. (2003)]
GLCM	correlation, contract, dissimilarity, energy, entropy, homogeneity, maximum probability.	[Kalyan, Jakhia, Lele, et al. (2014)]
NGTDM	busyness, contrast, complexity, coarseness, texture length	[Araki, Ikeda, Shukla, et al. (2016)]
IM	I1,I2,I3,I4,I5,I6,I7	[Yoshikawa, Ishii, Kurebayashi, et al. (2013)]
FD	H^1, H^2, H^3, H^4	[Christodoulou, Pattichis, Pantziaris, et al. (2003)] [Qiu, Chen, Li, et al. (2012)]
SP	eccentricity, perimeter, majoraxislength, minoraxislength	[Christodoulou, Pattichis, Pantziaris, et al.(2003)]

2.5 Statistical analysis

Initially, univariate linear regressions were performed between FCT measurements andvariables of IVOCT image features. Direct linear regression wasappropriate here, because the IVOCT images sampling interval was far more than 0.2 mm and the FCT measurements at nearby frameswere independent. In addition, multivariatelinear regressions were performed against all 32 image features.Multiple correlation coefficient between variables was estimated using Pearson's correlation coefficient (r). For all test, a two tailed p value<0.05 was considered

statistically significant. All statistical analysis was performed with SPSS statistical software (IBM SPSS Statistics for Windows, Version 19.0. IBM Corp, Armonk, New York).

3 Result

Table 2 reports statistically significant (*p*) and Pearson correlation coefficient (*r*) between univariate feature and mFCT(average twice measurements of FCT) measurements of 102 images. The correlation coefficient is generally low, where the lowest and highest values are 0.64 (mean and energy) and 0.05 (I4). Bold *p*-values represent no statistically significant between two variable values.

Table 2: The correlation coefficient of mFCT and univariate image features by two observers

	mFCT			mFCT	
feature name	*r*	*p*-value		*r*	*p*-value
mean	0.64	<0.001	Texture length	0.38	<0.001
variance	0.49	<0.001	I1	0.54	<0.001
median	0.48	<0.001	I2	0.22	0.03
skewness	0.51	<0.001	I3	0.33	<0.001
kurtosis	0.53	<0.001	I4	0.05	**0.59**
correlation	0.61	<0.001	I5	0.13	**0.19**
contract	0.61	<0.001	I6	0.28	<0.001
dissimilarity	0.62	<0.001	I7	0.50	<0.001
energy	0.64	<0.001	H^1	0.08	**0.43**
entropy	0.48	<0.001	H^2	0.08	**0.41**
homogeneity	0.35	<0.001	H^3	0.44	<0.001
maximum probability	0.34	<0.001	H^4	0.06	**0.56**
busyness	0.25	0.0112	eccentricity	0.27	<0.001
contrast	0.36	<0.001	perimeter	0.16	**0.10**
complexity	0.16	**0.10**	mal	0.26	0.01
coarseness	0.39	<0.001	mil	0.41	<0.001

Similarly, Table 3shows statistically significant (*p*) and Pearson correlation coefficient (*r*) between multivariate features and mFCT measurements. Statisticallysignificant results were observed in each group i.e. individual group feature setand the fusion feature set.

The lowest correlation coefficient of individual group appeared at shape parameter group (SP), whichwas 0.58 for observer. The phenomenon was in turn confirmed in Table 2 that the correlation coefficient of four shape parameters were overall lower than others.In the contrast, the highest correlation coefficient of individual group was observed in feature set 2 (GLCM),which were 0.80. Pearson correlation coefficient of the fusion feature sets were0.91, which better than any individual group feature set.

Table 3: The correlation coefficient of mFCTand multivariate image features

Feature set	mFCT	
	r	*p*-value
FOS	0.68	<0.001
GLCM	0.80	<0.001
NGTDM	0.74	<0.001
FD	0.72	<0.001
IM	0.62	<0.001
SP	0.58	<0.001
Fusion feature sets	0.91	<0.001

4 Discussion

FCT is important indicator of plaque vulnerability, thus could potentially guide appropriate surgical treatment such as percutaneous coronary intervention (e.g., balloon angioplasty or stent placement). The reliable examination of these indicators of atherosclerotic plaques will ultimately determine the clinical value of IVOCT images, depending on the application of meaningful and reproducible methods.The mainfindingsof the present study are the excellent inter-observer agreement of the manual assessment of FCT measurements with previous studies. In addition, the highcorrelation between the image features of segmented ROIs and FCT measured, which show that IVOCT image feature is able to provide more information in quantization FCT measurements to promote both the computer-aided routine clinical use and analysis of large-scale data sets from clinical trials in vulnerable plaque.

The current accepted universal method for assessing FCT measurements *in vivo* using IVOCT images is based on single measurement of the thinnest portion of the fibrous cap [Kubo, Imanishi, Takarada, et al. (2007);Kume, Akasaka, Kawamoto, et al. (2006)]. In practice, the extensive clinical image data *in vivo*were usually analyzed manually by expert analysts. Indeed, the excellent inter-observer agreement of IVOCT images to measure the FCT manually, have been previously reported. Kim et al. [Kim, Lee, Kato, et al. (2012)] performed first *in vivo* investigation in the inter-observer agreement (ICC=0.99) by 4 independent observers. Subsequently, Gerbaud et al [Gerbaud, Weisz, Tanaka, et al. (2016)] reported the excellent inter-observer agreement resulted for FCT

measurement, with ICC of 0.99 was reached in the analysis and was similar to literature previously. Greatly, excellentinter-observer agreement (ICC=0.99) was achieved for FCT measurement, consistent with the result of the previous mentioned studies.

Although others' and ourstudies had been certified the FCTmeasurements may be repeatable by independent observer manually,few literates focus on the interrelationship between IVOCT image features and FCT measurements.Such an idea will help in enhancing the significance of noninvasive coronary artery tests in the identification of FCT measurementsand assessment the risk factors of stroke. Thus, in the study, we first analyzedthe correlation coefficient and statistically significant between FCT measurementsandthe six group image features based on the priori knowledge that the more higher the correlation coefficient, the better elucidate the image features were used to quantify FCT.

The results in this study (Table 2 and Table 3) indicate significant relationships between image features and FCT measurements. The *r*value of the univariate regressions indicate that only several single texture feature factor are dominant in determining FCT, there are mean, contract, dissimilarity, energy, entropy, homogeneity, maximum probability (Table 2). On the other hand, the individual feature set of the multivariate regressions are all highly significant, and the correlation coefficients are substantially higher as well (Table 3). Thus, FCT measurements seem to be influenced by multiple aspects of the texture features and shape parameters. This is to be expected, the texture features are postulated to act through their influence on the spatial interrelationships and arrangementof the gray image, and it is reasonable that each of these FCT (the minimum distance implied in the spatial arrangement) would be influenced by texture feature and shape parameters.Best feature sets were the GLCM feature set, followed by the FD. In general, all individual feature set performed in a range of about 0.62-0.80, except of the shape parameters that performed much worse.In order to enhance the influences of feature set, the six feature sets were combined, by connecting the feature one by one. Fusing results of the six different feature sets, improved the correlation results obtained by the individual feature sets, reaching an average correlation coefficient of 0.91 for observer. The benefits of fusionresults are more obvious in the case where there is no dominant best feature sets, as the case with the features extracted from the lipid-rich plaque images in this study. It is noteworthy in this respect that the signs of the regression coefficients in the univariate and multivariate regressions in Tables 1 and 2 are consistent.

5 Study Limitations

In multivariate regression analysis, correlation among the independent variables is one common problem. The problem may be an influentialfactor if the primary purpose of the regression is to identify important explanatory variables that might play a causal role. The estimated regression coefficients for such correlated variables can be different. This problem was not involved and discussed in our case. Feature selection method with deleting the possible correlations between the independent variables are suggested in the future research.

In computer vision analysis, efficiency measured by the computational time is another

common problem. Computational times for preprocessing, lumen segmentation, scan-conversion and ROI segmentation were recorded bymatlab code, especially scan-conversion spent a long time (two hours for 271 images) in the study. As such, further coding and implementation in a faster language (e.g. C/C++) would significantly reduce computational time, possibly achieving the analysis of a multiple IVOCT images in a few minutes.

Lack of histology data as the golden standard in the FCT measurement is the third problem. Given that IVOCT manual FCT measurementsof atherosclerotic plaques are subject to some inter-observer variability, the use of a third reader is always required in case of disagreement between two readers. As a matter of fact, only FCT measurement using a large series of histological samples would be able to give more objective and detailed results.However, even if histology can provide a stronger ground truth, the correct registration with IVOCT images can be a challenge due to histological slice thickness and helicoidal IVOCT data acquisition [Rieber, Meissner, Babaryka, et al. (2006)]. Therefore, a large amount of histological data would be required to achieve enough statistical analysis result, which is not currently available.

7 Conclusion

We discussed the correlation between features and FCT measurementsin human coronary arteries based on IVOCT images. The regression result demonstrated the fusion feature played an important role in quantification FCT for online identification of high-risk plaques.

Acknowledgment: This study was partially supported by the National Natural Science Foundation of China (NSFC) (No. 11772093, 11272091, 11422222, 31470043), and ARC (FT140101152).

Compliance with ethical standards

Conflict of interest The authors declare that they have no conflict of interest.

Informed consent Informed consent was obtained from all individualparticipants included in the study.

Ethical approval All procedures performed in studies were in accordance with the ethical standards of the responsible committee on human experimentation (institutional and national) and with the Declaration of Helsinki 1975, as revised in 2008.

References

Araki, T.; Ikeda, N.; Shukla, D.; Jain, PK.; Londhe, ND.; Shrivastava, VK.; Banchhor SK.; Saba L.; Nicolaides A.; Shafique S.; Suri JS (2016): PCA-based polling strategy in machine learning framework for coronary artery disease risk assessment in intravascular ultrasound: a link between carotid and coronary grayscale plaque morphology. *Comput Methods Programs Biomed*, vol. 128, pp.137-158.

Athanasiou, L. S.; Bourantas, C. V.; Rigas, G.; Sakellarios, AI.; Exarchos, TP.;Siogkas, PK.; Ricciardi, A.; Naka, KK.; Papafaklis, MI.; Michalis, LK.; Prati, F.;

Fotiadis, DI.(2014): Methodology for fully automated segmentation and plaque characterization in intracoronary optical coherence tomography images. *J Biomed Opt* , 19 (2). 026009.

Bouma, BE.; Suter, MJ.; Shishkov, M.; Ughi, GJ.; Halpern, EF.; Rosenberg, M.; Waxman, S.; Moses, JW.; Mintz, GS.; Maehara, A.; Tearney, GJ. (2016): Multi-laboratory inter-institute reproducibility study of IVOCT and IVUS assessments using published consensus document definitions. *Eur Heart J Cardiovasc Imaging*, vol. 17, no. 7, pp.756-764.

Cardoso, L.; Weinbaum, S. (2014): Changing views of the biomechanics of vulnerable plaque rupture: a review. *Ann Biomed Eng*, vol. 42, no.2, pp. 415-431.

Chamie, D, Bezerra, HG.; Attizzani, GF.; Yamamoto, H.; Kanaya, T.; Stefano, GT.; Fujino, Y.; Mehanna, E.; Wang, W.; Abdul-Aziz, A.; Dias, M.; Simon, DL.; Costa, MA .(2013) : Incidence, predictors, morphological characteristics, and clinical outcomes of stent edge dissections detected by optical coherence tomography. *JACC Cardiovasc Interv*, vol.6, no. 8, pp. 800-813.

Christodoulou,CI.; Pattichis, CS.; Pantziaris, M.; Nicolaides, A.(2003):Texture-based classification of atherosclerotic carotid plaques. *IEEE Trans Med Imaging*, vol. 22, no. 7, pp. 902-912.

Di, Vito. L.; Yoon, JH.; Kato, K.; Yonetsu, T.; Vergallo, R.; Costa, M.; Bezerra, HG.; Arbustini, E.; Narula, J.; Crea, F.; Prati, F.; Jang, IK. (2014): Comprehensive overview of definitions for optical coherence tomography-based plaque and stent analyses. *Coron Artery Dis*, vol. 25, no.2, pp. 172-185.

Falk, E.; Nakano, M.; Bentzon, JF.; V.Finn, A.; Virmani, R. (2013) Update on acute coronary syndromes: the pathologists' view. *Eur Heart J*, vol. 34, no. 10, pp. 719-746.

Fujii, K.; Hao, H.; Shibuya, M.; Imanaka, T.; Fukunaga, M.;, Miki, K.; Tamaru, H.; Sawada, H.; Naito, Y.; Ohyanagi, M.; Hirotak, S.; Masuyama, T. (2015): Accuracy of OCT, grayscale IVUS, and their combination for the diagnosis of coronary TCFA: an ex vivo validation study. *JACC Cardiovasc Imaging*, vol. 8, no. 4, pp. 451-460.

Gerbaud, E.; Weisz, G.; Tanaka, A.; Kashiwagi, M.; Shimizu, Wang L.; Souza, C.;

Rieber, J.; Meissner, O.; Babaryka,G.; Reim,S.; Oswald,M.; Koenig,A.; Schiele TM.; Shapiro, M.; Theisen, K.; Reiser, MF.; Klauss, V.; Hoffmann, U. (2006): Diagnostic accuracy of optical coherence tomography and intravascular ultrasound for the detection and characterization of atherosclerotic plaque composition in ex-vivo coronary specimens: a comparison with histology. *Coron Artery Dis*, vol.17, no. 5, pp. 425-430.

Habara, M.; Nasu, K.; Terashima, M.; Ko, E.; Yokota, D.; Ito, T.; Kurita,T.; Teramoto, T.; Kimura, M.; Kinoshita, Y.; Tsuchikane, E.; Asakura, Y.; Matsubara, T.; Suzuki, T. (2014): Impact on optical coherence tomographic coronary findings of fluvastatin alone versus fluvastatin plus ezetimibe. *Am J Cardiol*, vol. 113, no.4, pp. 580-587.

Jang, IK.; Tearney, GJ.; MacNeill, B.; Takano M.; Moselewski, F.; Iftima, N.;Shishkov, M.; Houser, S.; Aretz, HT.; Halpern, EF.; Bouma, BE. (2005): In vivo characterization of coronary atherosclerotic plaque by use of optical coherence tomography.

Circulation, vol.111, no. 12, pp. 1551-1555.

Jang, IK.; Bouma, BE.; Kang, DH.; Park, SJ.; Park, SW.; Seung, KB.; Choi, KB.; Shishkov, M.; Schlendorf, K.; Pomerantsev, E.; Houser, SL.; Aretz, HT.; Tearney, GJ.(2002) :Visualization of coronary atherosclerotic plaques in patients using optical coherence tomography: comparison with intravascular ultrasound. *J Am Coll Cardiol* , vol.39, no. 4, pp. 604-609.

Kato, K.; Yonetsu, T.; Jia, HB.; Abtahian, F.; Vergallo, R.; Hu, SN.; Tian, JW.; Kim, SJ.; Lee, H.; McNulty, I.; Lee, S.; Uemura, S.; Jang, Y.; Park, SJ.; Mizuno, K.; Yu, B.; Jang, IK. (2013): Nonculprit coronary plaque characteristics of chronic kidney disease. *Circ Cardiovasc Imaging*, vol. 6, no 3, pp. 448-471.

Kalyan, K.; Jakhia, B.; Lele, RD.; Joshi, M.; Chowdhary, A (2014): Artificial neural network application in the diagnosis of disease conditions with liver ultrasound images. *Adv Bioinform*, vol.14, pp.14-28.

Kim, SJ.; Lee, H.; Kato, K.; Yonetsu, T.; Xing, L.; Zhang, S.; Jang, IK. (2012) Reproducibility of in vivo measurements for fibrous cap thickness and lipid arc by OCT. *JACC Cardiovasc Imaging*, vol.5, no.10, pp. 1072-1074.

Kini, AS.; Vengrenyuk, Y.; Yoshimura, T.; Matsumura, M.; Pena, J.; Baber, U.; Moreno, P.; Mehran, R.; Maehara, A.; Sharma, S.; Narula, J.(2017): Fibrous cap thickness by optical coherence tomography in vivo. *J Am Coll Cardiol*, vol. 69, no. 6, pp. 644-657.

Koga, S.; Ikeda, S.; Yoshida, T.; Nakata, T.; Takeno, M.; Masuda, N.; Koide, Y.; Kawano, H.; Maemura, K.(2013): Elevated levels of systemic pentraxin 3 are associated with thin-cap fibroatheroma in coronary culprit lesions assessment by optical coherence tomography and intravascular ultrasound. *JACC Cardiovasc Interv*, vol. 6, no. 9, pp. 945-954.

Kume, T.; Akasaka, T.; Kawamoto, T.; Okura, H.; Watanabe, N.; Toyota, E.; Neishi, Y.; Sukmawan, S.; Sadahira, Y.; Yoshida, K. (2006): Measurement of the thickness of the fibrous cap by optical coherence tomography. *Am Heart J*, vol. 152, no. 4, 755.e751–e754..

Kubo, T.; Imanishi, T.; Takarada, S.; Kuroi, A.; Ueno, S.; Yamano, T.; Matsuo, Y.; Masho, T.; Kitabata, H.; Tsuda, K.; Tomobuchi, Y.; Akasaka, T (2007): Assessment of culprit lesion morphology in acute myocardial infarction: ability of optical coherence tomography compared with intravascular ultrasound and coronary angioscopy. *J Am Coll Cardiol*, vol. 50, no.10, pp.933-939.

Meissner, OA.; Rieber, J.; Babaryka, G.; Oswald, M.; Reim, S.; Siebert, U.; Redel, T.; Reiser, M.; Mueller-Lisse, U. (2006): Intravascular optical coherence tomography: comparison with histopathology in atherosclerotic peripheral artery specimens.;*J VascIntervRadiol*, vol. 17, no. 2, pp. 343–349.

Prati, F.; Guagliumi, G.; Mintz, GS.; Costa, M.; Regar, E.; Akasaka, T.; Barlis, P.; Tearney, GJ.; Jang, IK.; Arbustini, E.; Bezerra, HG.; Ozaki, Y.; Bruining, N.; Dudek, D.; Radu, M.; Erglis, A.; Motreff, P.; Alfonso, F.; Toutouzas, K.; Gonzalo, N.;Tamburino, C.; Adriaenssens, T.; Pinto, F.; Serruys, PW.; Di Mario, C. (2012) : Expert review document part 2: methodology, terminology and clinical applications of

optical coherence tomography for the assessment of interventional procedures. *Eur Heart J*, vol. 33, no. 20, pp. 2513-2520.

Prati, F.; Regar, E.; Mintz, GS.; Arbustini, E.; Di, Mario C.; Jang, IK.; Akasaka, T.; Costa, M.; Guagliumi, G.; Ozaki, EG.; Pinto, F.; Serruys, PW. (2010): Expert review document on methodology, terminology, and clinical applications of optical coherence tomography: physical principles, methodology of image acquisition, and clinical application for assessment of coronary arteries and atherosclerosis. *Eur Heart J* , vol. 31, no. 4, pp. 401-415.

Qiu, WB.; Chen, Y.; Li, X.; Yu, YY.; Cheng, WF.; Tsang, FK.; Zhou, QF.; Shung, KK.; Dai, JY.; Sun, L (2012): An open system for intravascular ultrasound imaging. *IEEE Trans Ultrason Ferroelectr Freq Control*, vol. 59, no. 10, pp. 2201-2209.

Radu, MD.; Yamaji, K.; Garcia-Garcia, HM.; Zaugg, S.; Taniwaki, M.; Koskinas, KC.; Serruys, PW.; Windecker, S.; Dijkstra, J.; Raber, L.(2016): Variability in the measurement of minimum fibrous cap thickness and reproducibility of fibroatheroma classification by optical coherence tomography using manual versus semi-automatic assessment. *EuroIntervention*, vol. 12, no. 8, pp. 987-997.

Tanaka, A.; Imanishi, T.; Kitabata, H.; Kubo, T.; Takarada, S.; Tanimoto, T.; Kuroi, A.; Tsujioka, H.; Ikejima, H.; Komukai, K.; Kataiwa, H.; Okouchi, K.; Kashiwaghi, M.; Ishibashim, K.; Matsumoto, H.; Takemoto, K.; Nakamura, N.; Hirata, K.; Mizukoshi, M.; Akasaka, T. (2009): Lipid-rich plaque and myocardial perfusion after successful stenting in patients with non-ST-segment elevation acute coronary syndrome: an optical coherence tomography study. *Eur Heart J*, vol.30, no. 11, pp. 1348-1355.

Tearney, GJ.; Jang, IK.; Bouma, BE (2006): Optical coherence tomography for imaging the vulnerable plaque. *J Biomed Opt*, 11(2), 021002.

Tian, J.; Dauerman, H.; Toma, C.; Samady, H.; Itoh, T.; Kuramitsu, S.; Domei, T.; Jia, HB.; Vergallo, R.; Soeda, T.; Hu, SN.; Minami, Y.; Lee, H.; Yu, B.; Jang, IK. (2014): Prevalence and characteristics of TCFA and degree of coronary artery stenosis: an OCT.; IVUS, and angiographic study. *J Am Coll Cardiol*, vol. 64, no. 7, pp. 672-680.

Virmani, R.; Burke AP.; Farb A.; Kolodgie FD (2006): Pathology of the vulnerable plaque. *J Am Coll Cardiol*, vol. 47, no. 8 Suppl, pp. 13-18.

Wang, Z.; Chamie, D.; Bezerra, HG.; Yamamoto, H.; Kanovsky, J.; Wilson, DL.; Costa, MA.; Rollons, AM. (2012): Volumetric quantification of fibrous caps using intravascular optical coherence tomography. *Biomed Opt Express*, vol. 3, no. 6, pp. 1413-1426.

Wang, ZZ.; Liu, NN.; Zhang, LF.; Li, XY.; Han, XS.; Peng, YQ.; Dang, MZ.; Sun, LT.; Tian, JW.(2016): Real-time elastography visualization and histopathological characterization of rabbit atherosclerotic carotid arteries. *Ultrasound Med Biol*, vol. 42, no.1, pp. 176-184.

Yonetsu, T.; Kakuta, T.; Lee, T.; Takahashi, K.; Kawaguchi, N.; Yamamoto, G.; Koura, K.; Hishikari, K.; Iesaka, Y.; Fujiwara, H.; Isobe, M. (2011) : In vivo critical fibrous cap thickness for rupture-prone coronary plaques assessed by optical coherence tomography. *Eur Heart J*, vol.32, no.10, pp.1251-1259.

Yoshikawa D.; Ishii H.; Kurebayashi N.; Sato B.; Hayakawa S.; Ando H.; Hayashi M.; Isobe S.; Okumura T.; Hirashiki A.; Takeshita K.; Amano T.; Ueteni T.; Yamada S.; Murohara T (2013): Association of cardiorespiratory fitness with characteristics of coronary plaque: Assessment using integrated backscatter intravascular ultrasound and optical coherence tomography. *Int J Cardiol*, vol. 162, no. 2, pp. 123-128.